Revista ALCONPAT
www.revistaalconpat.org
eISSN 2007-6835
Revista de la Asociación Latinoamericana de Control de Calidad, Patología y Recuperación de la Construcción

Numerical analysis of the effect of variation of eccentricity of unbonded post-tensioned tendons on the structural behavior of flat slabs

R. Cattelan[1]*, L. Cielo[1], A. Lübeck[1], A. B. S. Santos Neto[1]
*Contact author: rogerio@ufsm.br
DOI: https://doi.org/10.21041/ra.v12i2.570

Reception: 11/11/2021 | Acceptance: 26/02/2022 | Publication: 01/05/2022

ABSTRACT

In this study, the effect of variations of eccentricity of tendons in unbonded post-tensioned flat slabs was evaluated. The correct positioning of strands in the assembly of unbonded post-tensioned flat slabs is essential for the structural system to achieve adequate performance and safety. Four different slab models were analyzed with variations in the height of the strands at different positions providing the change in eccentricity and increases in the number of tendons. Pre-compression stresses, stresses on the bottom and top faces, center vertical displacements, load balancing and passive reinforcement of the slabs were evaluated. The ADAPT Floor Pro commercial software was used for the analyses with the design conforming with standard NBR 6118:2014 and recommendations from standard ACI 318:2019. For the models evaluated, it was found that the variation in the eccentricity of the strands in the bottom face of the slab reduced the applied stresses more than variations in the top face.

Keywords: post-tensioned concrete, unbonded tendons, strand eccentricity.

Cite as: Cattelan, R., Cielo, L., Santos Lübeck, A., Neto, A. B. S. (2022), "*Numerical analysis of the effect of variation of eccentricity of unbonded post-tensioned tendons on the structural behavior of flat slabs*", Revista ALCONPAT, 11 (2), pp. 210 – 226, DOI: https://doi.org/10.21041/ra.v12i2.570

[1] Universidade Federal de Santa Maria, Av. Roraima nº 1000 Cidade Universitária Bairro - Camobi, Santa Maria - RS, 97105-900, Brazil.

Contribution of each author
All authors contributed equally in the conception and definition of the methodology. Author Cielo contributed to the numerical model (100%), analysis and discussion of results (25%) and writing (100%). Author Lima contributed with advising (50%), analysis and discussion of results (25%) and proofreading (34%). Author Santos Neto contributed with advising (50%), analysis and discussion od results (25%) and proofreading (33%). Author Lübeck contributed with analysis and discussion of results (25%) and proofreading (33%).

Discussions and subsequent corrections to the publication
Any dispute, including the replies of the authors, will be published in the first issue of 2023 provided that the information is received before the closing of the third issue of 2022.

Revista ALCONPAT, 12 (2), 2022: 210 – 226

Análise da influência da variação da excentricidade de cordoalhas engraxadas no comportamento estrutural de lajes lisas protendidas

RESUMO

Neste estudo, avaliou-se a influência de variações de excentricidade dos cabos em lajes lisas protendidas. O correto posicionamento das cordoalhas na montagem de lajes lisas protendidas é imprescindível para que o sistema estrutural alcance desempenho e segurança adequados. Analisou-se quatro modelos diferentes com modificação da altura dos cabos em diferentes pontos e quantidades. Foram avaliadas tensões de pré-compressão, tensões nas faces inferior e superior, flechas, balanceamentos de cargas e armaduras passivas. Utilizou-se o programa ADAPT Floor Pro para as análises, sendo o dimensionamento regido pela NBR 6118:2014 e recomendações do ACI 318:2019. Constatou-se que a variação na excentricidade vertical das cordoalhas na face inferior da laje, reduzem mais os valores das tensões, em comparação com a variação na face superior.

Palavras-chave: Concreto Protendido, Protensão Não Aderente, Excentricidade de Cordoalhas.

Análisis de la influencia de la variación de excentricidad de tendones no-adherentes en el comportamiento estructural de losas planas postensadas

RESUMEN

En este estudio se evaluó la influencia de las variaciones de excentricidad de los cables en modelos con losas planas postensadas. El correcto posicionamiento de los tendones en el montaje de losas planas postensadas es fundamental para que el sistema estructural logre un adecuado rendimiento y seguridad. Se analizaron cuatro modelos arquitectónicos diferentes con modificación de la altura de los cables en diferentes puntos y cantidad. Se evaluaron tensiones de pre compresión, tensiones extremas en el tope y base, desplazamientos verticales, balanceo de carga y cantidad de acero pasivo de las losas. Para el análisis se utilizó el software ADAPT Floor Pro. El proyecto sigue las recomendaciones de la NBR 6118:2014 y ACI 318:2019. Para los modelos evaluados, se encontró que la variación en la excentricidad vertical de los tendones en la base de la losa reduce aún más los valores de las tensiones aplicadas, en comparación con la variación en el tope.

Palabras clave: hormigón postensado; postensión no-adherente; excentricidad de los tendones.

1. INTRODUCTION

The use of unbonded tendons in building construction is frequent in developed countries like the USA and Australia, as well as parts of the Middle East, Southeast Asia, United Kingdom and in some South American countries. The choice of its use is due to excellent structural performance and economic advantages (Aalami, 2000; Santos, 2017; Silva *et al*., 2018).

Unbonded tendons were included in standard ACI 318 of the American Concrete Institute from 1963 and onwards after its use in several construction projects around the world (Aalami, 2000; Kang and Bondy, 2008). In Brazil, the use of unbonded tendons in post-tensioned flat slabs started only in 1997 (Carvalho, 2017). This was partially driven by architectural designs with wide spans and reduced number of pillars and beams in upscale residential buildings (Santos, 2017; Almeida, 2001; Loureiro, 2006). Other decisive factors that promoted the effective application of post-tension concrete in civil construction were the development of high strength steel, advancements in design software and its relative ease of execution (Carvalho, 2017; Loureiro, 2006).

Prestressing has economic benefits and improves performance throughout the projected service life (PSL) and structural safety of concrete. In particular, it improves durability as the prevention or decrease in fissuring inhibits corrosion and ensures greater protection to the reinforcement (NBR 6118, 2014; Cholfe and Bonilha, 2018; Silva, 2003).

In flat slabs with post-tensioned unbonded tendons, the strands are usually placed in a parabolic arch which produces an eccentricity with respect to the center of the slab. This allows an increase in the loads applied to the strands and also increases the load balancing capacity (Pfeil, 1984; Vicente and Albino, 1994). The basic principle of load balancing is to allow the vertical portion of the tendons stress to balance out part of the dead load and result in a structure subjected only to compressive stresses (Silveira, 2002; Aalami, 1990; Aalami and Bommer, 1999). In order to accomplish this, vertical tendon placement must be as close as possible as projected. Incorrect vertical placement could lead to negative consequences such as different center deflection from predicted values and, in more severe cases, even structural collapse (Silva *et al*., 2018; Aalami and Bommer, 1999; Romanichen and Souza, 2019).

In order to ensure vertical strand placement in accordance to projected values, spacers are used in regular intervals. Mass-produced spacers are made from plastic or steel with rigorous quality control with respect to height. However, in some exceptional cases, spacers are manufactured *in situ* with folded steel bars and inadequate quality control, resulting in variations in height (Loureiro, 2006; Aalami, 2014). Furthermore, other factors such as improper handling of the reinforcement or damage to it during pouring of concrete can lead to breaking or displacement of spacers as shown in Figure 1. Even with proper quality control, there is a human factor that can result in incorrect placement of spacers during tendon assembly. The end result of all these factors are strands placed at heights and eccentricities different than projected.

The incorrect placement of strands can lead to slab fissuring, excessive vertical displacements and loading stresses different from predicted to the point of exceeding projected limits of tension and compression in the structural element. Further effects can occur such as concrete flaking and acceleration of steel corrosion due to insufficient cover (Souza, 2018; Xin and Xianyan, 2012).

(a) (b)

Figure 1. Concrete pouring example: (a) workers in direct contact with the reinforcement and (b) damaged and out of position spacer.

The correct vertical positioning of strands in accordance with projected values during the assembly stage has been cited as the main factor affecting system performance (Carvalho, 2017; Souza Junior and Oliveira, 2016; Caro *et al*., 2013). Cauduro (2002) recommended a maximum tolerance of +/- 5 mm in vertical variations of stand placement for slabs of less than 200 mm thick and +/- 10 mm for slabs between 200 mm and 600 mm thick. The most critical locations were the low and high points in the curvature, while horizontal position was not as crucial but excessive variation should be avoided. However, acceptable variations in absolute deviation, which were independent of structural geometry and applied loads, could still lead to an unsafe structural condition. Variations in tendon eccentricity could have an effect depending on slab thickness, relative eccentricity error, span width between pillars and applied load.

This study evaluated the effect of variations in eccentricity of tendons in flat, post-tensioned slabs. Several models were tested with different spans and relative error in eccentricity. The post-tensioned slabs were projected in accordance with standard ABNT NBR 6118:2014 and recommendations from ACI 318:2019.

2. METHODOLOGY

2.1 Slab Geometry and Strand Layout

The structural models consisted of a single slab supported directly by pillars and without beams as shown in Figure 2. The span between pillars was constant for each model. Four models were manufactured with spans of 7.0 m x 7.0 m to 10.0 x 10.0 m in 1 m increments and were designated M7, M8, M9 and M10. The slab thickness varied for each model and were defined approximately as L/42 (ACI 318, 2019), where L is the span between pillars. The characteristics of each model are shown in Table 1.

Strand layout concentrated tendons along the larger direction (in this case, Strands 1 through 3 in the x-direction) and a more regular distribution was applied in the perpendicular direction (in this case, Tendons 1 through 27 in the y-direction) as seen in Figure 3. The analyses were exclusive to central Strand 2 in the x-direction since it concentrated the most loads and should be the most affected by variations in eccentricity of each model. The number of tendons in central Strand 2 for models M7, M8, M9 and M10 were 10, 17, 25 and 33, respectively. Also shown in Fig.3 are the locations of the pillars, labeled P1 through P12.

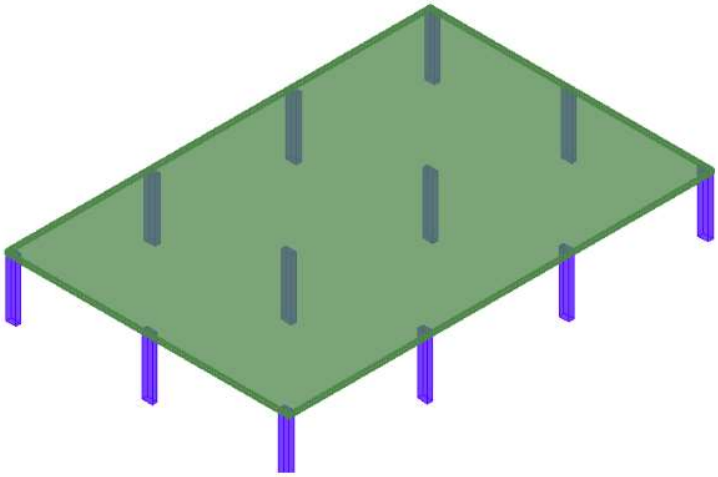

Figure 2. Sample structural model of post-tensioned slab for analysis.

Table 1. Model designations and dimensions

	Designation	Span between pillars	Slab thickness
Model	M7	7.0 m x 7.0 m	170 mm
	M8	8.0 m x 8.0 m	190 mm
	M9	9.0 m x 9.0 m	210 mm
	M10	10.0 m x 10.0 m	240 mm

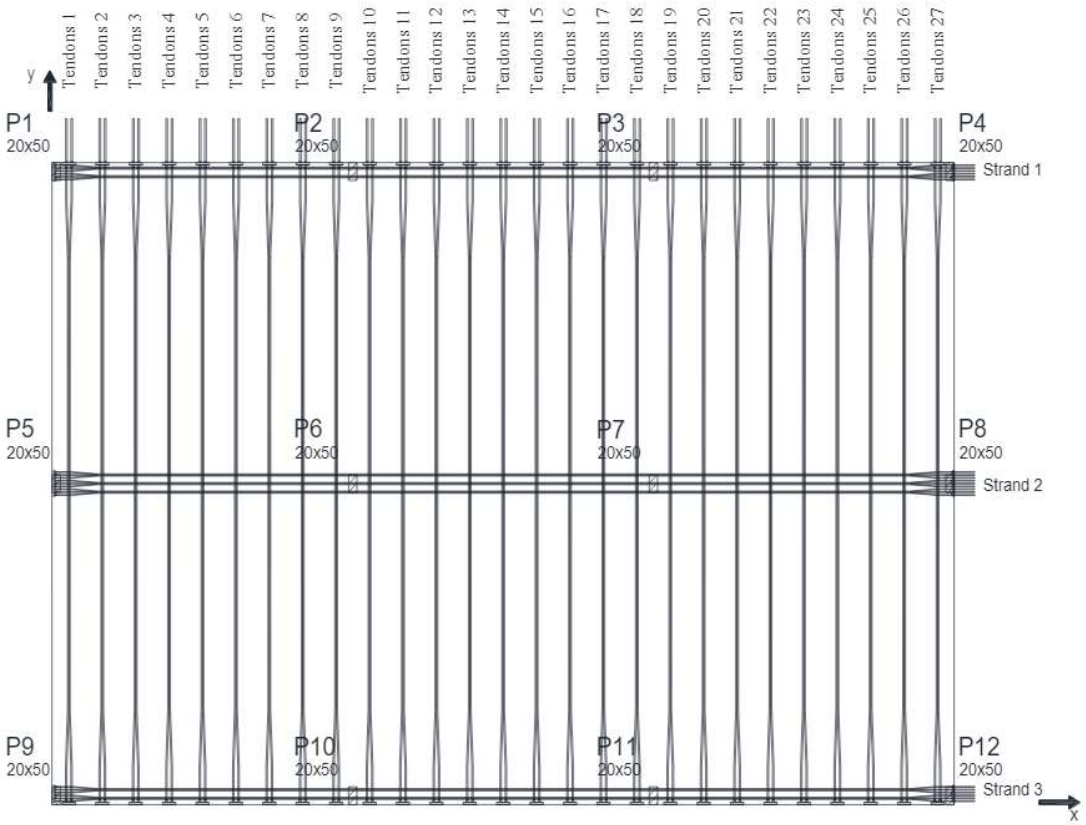

Figure 3. Layout of unbonded tendons and strands in a model post-tensioned slab.

Revista ALCONPAT, 12 (2), 2022: 210 – 226

The variations in eccentricity are shown schematically in Figure 4. Concave down eccentricities curving towards the top of the slab were placed on locations above pillars while concave up eccentricities towards the bottom of the slab were placed in the span between pillars. Three test cases of variation of eccentricity were tested. In the first case, only concave down eccentricity (designated "Top") was reduced over pillars P6 and P7. In the second case, only concave up eccentricity in was reduced in the span between pillars (designated "Bottom"). In the third case, a simultaneous decrease in eccentricity in both locations was applied in order to obtain a critical combination (designated "Critical").

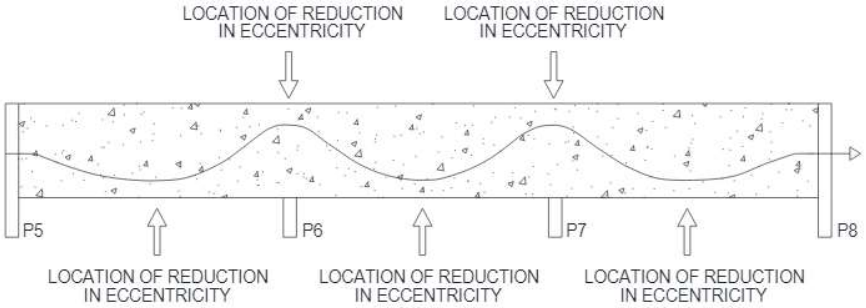

Figure 4. Variation of eccentricity along center Strand 2 and locations of reduction of eccentricity.

A total of 4 variations of eccentricity were applied to each of the 4 models shown in Table 1, designated hypothesis H1 through H4. The variations in eccentricity were of 5 mm, 10 mm, 15 mm and 20 mm. These variations were selected because projected spacer heights are usually listed in 5 mm increments and it would also allow easier and practical verification *in loco*. Additionally, Cauduro (2002) established that decreases in eccentricity should be limited to 5 mm and 10 mm for slab thicknesses equal or larger than the ones of this study. The variations of eccentricity and their designations are shown in Table 2.

Table 2. Designations of variations in eccentricity of this study.

Variation	Designation	Decrease in eccentricity (mm)
Reference	H0	0
Hypothesis 1	H5	5
Hypothesis 2	H10	10
Hypothesis 3	H15	15
Hypothesis 4	H20	20

For the analysis, the spans with decreased eccentricity were labeled "First" between P5 and P6, "Central" between P6 and P7 and "Final" between P7 and P8. These are shown in Figure 5.

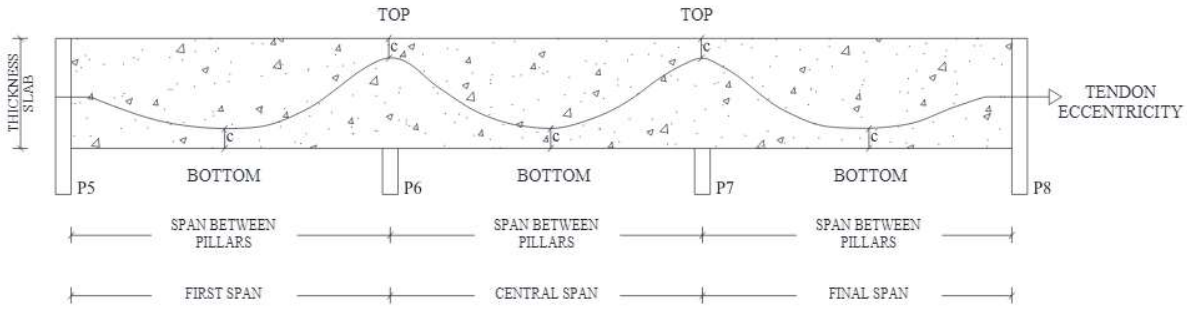

Figure 5. Designation of spans with variations of eccentricity.

2.2 Materiais and Reference Parameters

Concrete covers were 2.5 cm for slabs with passive reinforcements and 3.0 cm for active reinforcements. In the numerical models, a C35 class concrete was adopted with a f_{ck} of 35.0 MPa and modulus of elasticity (E) of 39.7 GPa. The tendons used were CP 190 RB (f_{ptk} = 1,900 MPa), nominal diameter of 12.7 mm and nominal steel area of 100.9 mm².

A variable (over)load of 2.5 kN/m² was applied to the slab, which corresponded to the minimum value recommended in standard NBR 6120 (ABNT, 2019). A dead load consisting of the structure's own weight based on slab thickness and a permanent load of 1.0 kN/m² representing other materials was also present.

The numerical analysis considered three fundamental parameters: minimum pre-compression strength, tensile normal stress limit and maximum vertical displacement. Other criteria such as load balance and final displacements were adjusted once these fundamental parameters were reached. Afterwards, the slabs were loaded in order to test projected service life (PSL) and useful service life (USL). The pre-compression stress at any point in the slab was kept at a minimum of 1.0 MPa in accordance with ACI 318 (ACI, 2019) and NBR 6118 (ABNT, 2014). In pre-testing, models in which the pre-compression stress of 1.0 MPa was insufficient to produce the tensile normal stress limit or maximum vertical displacements, the number of tendons was increased until these parameters were reached.

Whenever possible, a load balance parameter between 60% and 80% of the permanent load was adopted. This range of values was commonly used in slabs of residential and commercial buildings and parking garages (Loureiro, 2006).

A limited stress was defined in accordance with standard NBR 6118 (ABNT, 2014). As described, the tension stress of a flat slab was defined as sufficient for fissure formation at PSL (f-PSL) from a combination of loads under any class of environmental aggression. In this case, the normal compressive stress applied to the concrete when stressing was limited to 15.75 MPa while the f-PSL threshold stress was 21.0 MPa in accordance with standard ACI 318 (ACI, 2019).

Standard NBR 6118 (ABNT, 2014) defined minimum measurable vertical displacements in beams and slabs as L/250, where L is the span in between pillars. This value was used as a limit in the numerical models before variations in eccentricity of the strands were introduced. After the variations in eccentricity were introduced, analyses were performed to confirm which models were still within limits. Through this methodology, passive reinforcements, strand placement and maximum acceptable strand eccentricity were determined for each model. Passive bottom and top reinforcements were determined for the models based on criteria from standard NBR 6118 (ABNT, 2014). The combined criteria and limits used in the slabs are presented in Table 3.

2.3 Slab Analysis

Slabs were analyzed with Adapt Floor 2017 PRO commercial software. This program specialized in the design and analysis of post-tensioned concrete structures with a finite element method. The program evaluated the effects of post-tensioning in accordance with geometry and loading on the strands.

Adapt Floor 2017 PRO provided automatic mesh generation with user input on the size of elements. Two maximum element sizes were tested in this study and the results showed no significant differences. Consequently a maximum element size of 500 mm was used for all analyses. A sample mesh for model M8 is shown in Figure 6.

Table 3. Model criteria and limits with references.

Criteria	Limit	Parameter	Units	Reference
Pre-compression stress	Minimum	1.0	MPa	NBR 6118, ACI 318
Top and bottom tensile stress	Maximum	3.38	MPa	NBR 6118
Maximum compression stress at post-tensioning	Maximum	15.0	MPa	ACI 318
Maximum compression stress for f-PSL	Maximum	21.0	MPa	ACI 318
Load balance	Recommended	60 a 80	%	Loureiro (2006), Hanai (2005)
Vertical displacement	Maximum	L/250	-	NBR 6118

Slab model analysis made use of support lines aligned with pillar positions. Each support line defined "design sections" with average stress values which compiled stresses from surrounding areas delimitated by the support lines.

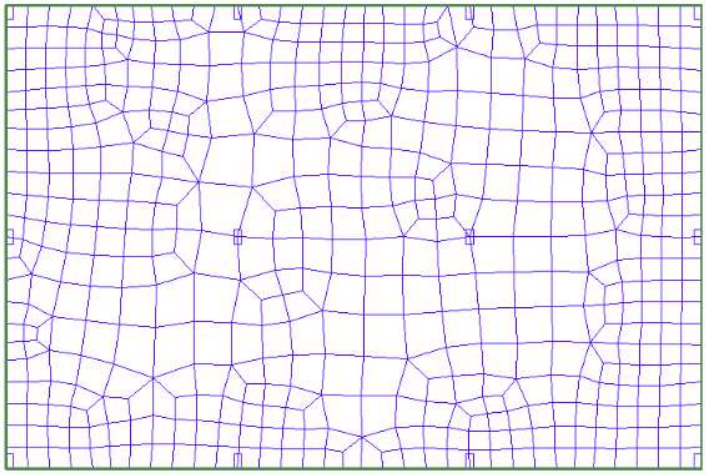

Figure 6. Finite element mesh for slab model M8.

Figure 7 shows normal stresses in the x-direction on the top and bottom faces of the slab for the most frequent combination in model M8.

3. RESULTS AND DISCUSSION

3.1 Pre-compression stresses

Table 4 presents pre-compression normal stress values on the slabs. No variations in stress were identified with respect to changes in the vertical position of the strands but rather with respect to the number of tendons and applied load. As the span between pillars increased, an increasing number of tendons were necessary to balance the models, resulting in a corresponding increase in pre-compression stress. The shortest span Model M7 presented stresses in between 1.0 MPa and 1.11 MPa while the longest span Model M10 had stresses between 1.43 MPa and 1.60 MPa.

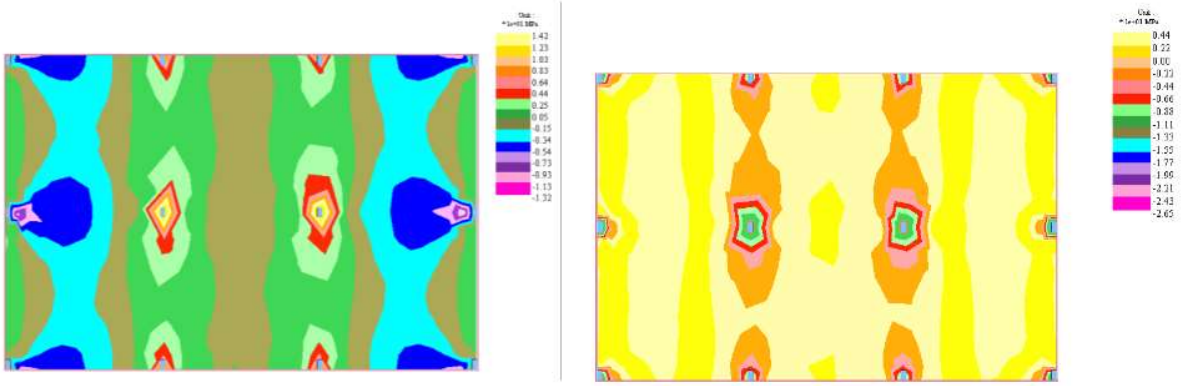

(a) Top face (b) Bottom face

Figure 7. Normal stresses in the x-direction for slab model M8 (MPa).

Table 4. Pre-compression normal stresses on the slab (MPa).

Model		M7											
Case		Reference	Top				Bottom				Critical			
Hypothesis			H5	H10	H15	H20	H5	H10	H15	H20	H5	H10	H15	H20
Span	Primeiro	1.00	1.00	1.00	1.00	1.00	1.00	1.00	1.00	1.00	1.00	1.00	1.00	1.00
	Central	1.11	1.11	1.11	1.11	1.11	1.11	1.11	1.11	1.11	1.11	1.11	1.11	1.11
	Último	1.01	1.01	1.01	1.01	1.01	1.01	1.01	1.01	1.01	1.01	1.01	1.01	1.01
Modelo		M8												
Stress		Reference	Top				Bottom				Critical			
Hypothesis			H5	H10	H15	H20	H5	H10	H15	H20	H5	H10	H15	H20
Span	First	1.27	1.27	1.27	1.27	1.27	1.27	1.27	1.27	1.27	1.27	1.27	1.27	1.27
	Central	1.36	1.36	1.36	1.36	1.36	1.36	1.36	1.36	1.36	1.36	1.36	1.36	1.36
	Last	1.31	1.31	1.31	1.31	1.31	1.31	1.31	1.31	1.31	1.31	1.31	1.31	1.31
Model		M9												
Case		Reference	Top				Bottom				Critical			
Hypothesis			H5	H10	H15	H20	H5	H10	H15	H20	H5	H10	H15	H20
Span	First	1.53	1.53	1.53	1.53	1.53	1.53	1.53	1.53	1.53	1.53	1.53	1.53	1.53
	Central	1.75	1.75	1.75	1.75	1.75	1.75	1.75	1.75	1.75	1.75	1.75	1.75	1.75
	Last	1.53	1.53	1.53	1.53	1.53	1.53	1.53	1.53	1.53	1.53	1.53	1.53	1.53
Model		M10												
Case		Reference	Top				Bottom				Critical			
Hypothesis			H5	H10	H15	H20	H5	H10	H15	H20	H5	H10	H15	H20
Span	First	1.43	1.43	1.43	1.43	1.43	1.43	1.43	1.43	1.43	1.43	1.43	1.43	1.43
	Central	1.60	1.60	1.60	1.60	1.60	1.60	1.60	1.60	1.60	1.60	1.60	1.60	1.60
	Last	1.50	1.50	1.50	1.50	1.50	1.50	1.50	1.50	1.50	1.50	1.50	1.50	1.50

3.2 Maximum normal stresses on the slab

Normal tensile stresses on the bottom face of the slab are shown in Table 5 for all models. Despite changes to eccentricity through vertical position of the strands, all models were within the maximum limit of 3.38 MPa for f-PSL set by standard NBR 6118 (ABNT, 2014). In the case of the "Central" span of the Reference model, compressive stresses were found on the bottom face of the slab due to higher prestresses when compared to the "First" and "Final" spans. Less variation in stresses were observed for the variations of eccentricity of the "Top" cases when compared to the "Bottom" cases. Still, "Critical" combination cases produced the most unfavorable stresses.

Revista ALCONPAT, 12 (2), 2022: 210 – 226

Results for the stresses in the top face of the slab are summarized in Table 6. Stresses that exceeded the limit set by standard NBR 6118 (ABNT, 2014) were highlighted in yellow. Only stresses of the "Top" cases and hypothesis H5 were within the limit of 3.38 MPa. Decreases in eccentricity of the "Bottom" cases produced a greater increase in normal tensile stresses along the top face of the slab, especially in the regions supported by the pillars when compared to other locations. Models M7 and M9 with hypothesis H5 were the only slabs in which variations of eccentricity of the "Bottom" cases had normal tensile stresses lower than the limit of 3.38 MPa. Furthermore, no normal stresses for the most frequent "Critical" combination cases in all hypotheses of variations in eccentricity were below the 3.39 MPa limit for f-PLS.

Table 5. Normal tensile stresses at the bottom face of the slabs (MPa).

Model		**M7**											
Case		**Reference**	**Top**				**Bottom**				**Critical**			
Hypothesis			**H5**	**H10**	**H15**	**H20**	**H5**	**H10**	**H15**	**H20**	**H5**	**H10**	**H15**	**H20**
Span	**First**	2.37	2.39	2.42	2.45	2.47	2.45	2.54	2.63	2.72	2.48	2.60	2.71	2.83
	Central	-0.15	-0.12	0.00	0.05	0.12	-0.10	0.00	0.02	0.05	-0.03	0.09	0.22	0.36
	Final	2.52	2.55	2.58	2.60	2.63	2.61	2.69	2.78	2.86	2.63	2.75	2.86	2.97
Model		**M8**											
Case		**Reference**	**Top**				**Bottom**				**Critical**			
Hypothesis			**H5**	**H10**	**H15**	**H20**	**H5**	**H10**	**H15**	**H20**	**H5**	**H10**	**H15**	**H20**
Span	**First**	2.52	2.55	2.71	2.74	2.77	2.66	2.76	2.87	2.98	2.68	2.83	2.97	3.12
	Central	-0.62	-0.5	-0.5	-0.4	-0.3	-0.6	-0.5	-0.4	-0.4	-0.5	-0.3	-0.2	0.01
	Final	2.48	2.51	2.54	2.57	2.61	2.58	2.69	2.79	2.9	2.62	2.75	2.89	3.03
Model		**M9**											
Case		**Reference**	**Top**				**Bottom**				**Critical**			
Hypothesis			**H5**	**H10**	**H15**	**H20**	**H5**	**H10**	**H15**	**H20**	**H5**	**H10**	**H15**	**H20**
Span	**First**	2.64	2.65	2.71	2.74	2.77	2.66	2.76	2.87	2.98	2.68	2.83	2.97	3.12
	Central	-1.49	-1.4	-1.3	-1.2	-1.1	-1.3	-1.2	-1.1	-1	-1.2	-1	-0.8	-0.6
	Final	2.63	2.66	2.72	2.74	2.78	2.67	2.79	2.9	3.01	2.71	2.82	3.01	3.16
Model		**M10**											
Case		**Reference**	**Top**				**Bottom**				**Critical**			
Hypothesis			**H5**	**H10**	**H15**	**H20**	**H5**	**H10**	**H15**	**H20**	**H5**	**H10**	**H15**	**H20**
Span	**First**	2.70	2.73	2.77	2.80	2.83	2.81	2.91	3.01	3.12	2.84	2.97	3.10	3.24
	Central	-1.41	-1.33	-1.24	-1.15	-1.07	-1.34	-1.27	-1.20	-1.13	-1.26	-1.10	-0.93	-0.77
	Final	2.69	2.73	2.76	2.79	2.82	2.80	2.90	3.01	3.11	2.83	2.97	3.10	3.24

Table 6. Normal tensile stresses at the top face of the slabs (MPa).

Model		M7											
Case		Reference	Top				Bottom				Critical			
Hypothesis			H5	H10	H15	H20	H5	H10	H15	H20	H5	H10	H15	H20
Span	P5	3.04	3.12	3.21	3.29	3.37	3.15	3.25	3.36	3.46	3.23	3.42	3.61	3.80
	P6	3.26	3.33	3.41	3.48	3.56	3.36	3.45	3.55	3.65	3.43	3.61	3.78	3.96
Model		M8											
Case		Reference	Top				Bottom				Critical			
Hypothesis			H5	H10	H15	H20	H5	H10	H15	H20	H5	H10	H15	H20
Span	P5	3.28	3.38	3.47	3.56	3.65	3.40	3.52	3.65	3.77	3.50	3.71	3.93	4.14
	P6	3.08	3.18	3.28	3.37	3.47	3.21	3.33	3.46	3.58	3.30	3.53	3.75	3.97
Model		M9											
Case		Reference	Top				Bottom				Critical			
Hypothesis			H5	H10	H15	H20	H5	H10	H15	H20	H5	H10	H15	H20
Span	P5	3.09	3.19	3.29	3.40	3.51	3.24	3.34	3.42	3.55	3.26	3.49	3.72	3.95
	P6	3.13	3.22	3.31	3.45	3.53	3.29	3.42	3.56	3.57	3.39	3.64	3.88	4.12
Model		M10											
Case		Reference	Top				Bottom				Critical			
Hypothesis			H5	H10	H15	H20	H5	H10	H15	H20	H5	H10	H15	H20
Span	P5	3.28	3.37	3.47	3.56	3.66	3.40	3.52	3.65	3.77	3.50	3.71	3.93	4.15
	P6	3.23	3.32	3.42	3.52	3.65	3.33	3.47	3.65	3.77	3.45	3.67	3.88	4.11

3.3 Vertical Displacements Deslocamentos verticais

Table 7 presents vertical displacements for the model slabs. Models M7 and M8 had displacements of 28.0 mm and 32.0 mm, respectively. These displacements occurred for all hypotheses and were within the limits set by standard NBR 6118 (ABNT, 2014). For all variations in eccentricity in the "Top" case, model M9 had displacements lower than 36 mm only in the "Central" span while Model M10 had displacements of less than 40.0 mm. Both of these values were limits set by standard NBR 6118 (ABNT, 2014)

Revista ALCONPAT, 12 (2), 2022: 210 – 226

Table 7. Vertical displacements on all model slabs (mm).

Model		M7											
Case		Reference	Top				Bottom				Critical			
Hypothesis			H5	H10	H15	H20	H5	H10	H15	H20	H5	H10	H15	H20
Span	First	18.5	18.8	19.0	19.2	19.4	19.1	19.6	20.1	20.7	19.3	20.0	20.8	21.5
	Central	5.4	5.8	6.3	6.6	7.0	5.7	6.0	6.3	6.6	6.1	6.9	7.5	8.2
	Final	19.1	19.3	19.4	19.6	19.8	19.6	20.1	20.6	21.1	19.8	20.4	21.1	21.8
Model		M8											
Case		Reference	Top				Bottom				Critical			
Hypothesis			H5	H10	H15	H20	H5	H10	H15	H20	H5	H10	H15	H20
Span	First	24.2	24.4	24.7	24.9	25.2	24.9	25.6	26.3	27.0	25.1	26.1	27.2	28.0
	Central	4.8	5.1	5.5	6.5	7.1	5.3	5.6	6.1	7.1	5.8	6.7	7.7	8.7
	Final	23.9	24.2	24.6	24.8	25.1	24.7	25.5	26.3	30.0	25.0	26.1	27.1	28.1
Model		M9											
Case		Reference	Top				Bottom				Critical			
Hypothesis			H5	H10	H15	H20	H5	H10	H15	H20	H5	H10	H15	H20
Span	First	35.7	35.9	36.5	36.8	37.1	36.1	36.7	37.0	37.9	36.3	36.8	37.9	39.2
	Central	5.0	5.8	6.6	7.4	8.1	6.5	7.1	7.6	8.3	7.3	8.4	9.7	10.9
	Final	35.6	35.9	36.2	36.7	37.0	36.0	36.3	36.8	37.6	36.1	36.5	37.7	39.0
Model		M10											
Case		Reference	Top				Bottom				Critical			
Hypothesis			H5	H10	H15	H20	H5	H10	H15	H20	H5	H10	H15	H20
Span	First	35.4	35.7	36.4	38.0	39.0	36.3	37.2	38.1	40.1	36.9	39.3	41.6	42.5
	Central	2.7	3.3	5.0	8.9	10.1	3.3	5.9	9.0	10.3	4.0	6.6	9.9	12.0
	Final	34.8	35.2	35.9	37.4	38.3	35.8	36.7	37.6	39.6	36.1	38.9	40.0	42.1

The effects of changes in eccentricity on displacement are better understood graphically from Figure 8. In the figure, the vertical axis contained the f/L ratio, which represented the equivalent center span displacement in denominator format: for example L/430 with L/250 being the limit. The horizontal axis contained the relative eccentricities, which were the variation in height of the strand (eccentricity) with respect to slab thickness. The dashed lines were placed in order to visually separate the slab models. The relative eccentricity (or its variation) could have more or less of an effect depending on the case study: examining the trends of Figure 8, it could be noted that, for all slab models, the "Critical" hypothesis produced the most variations in displacement.

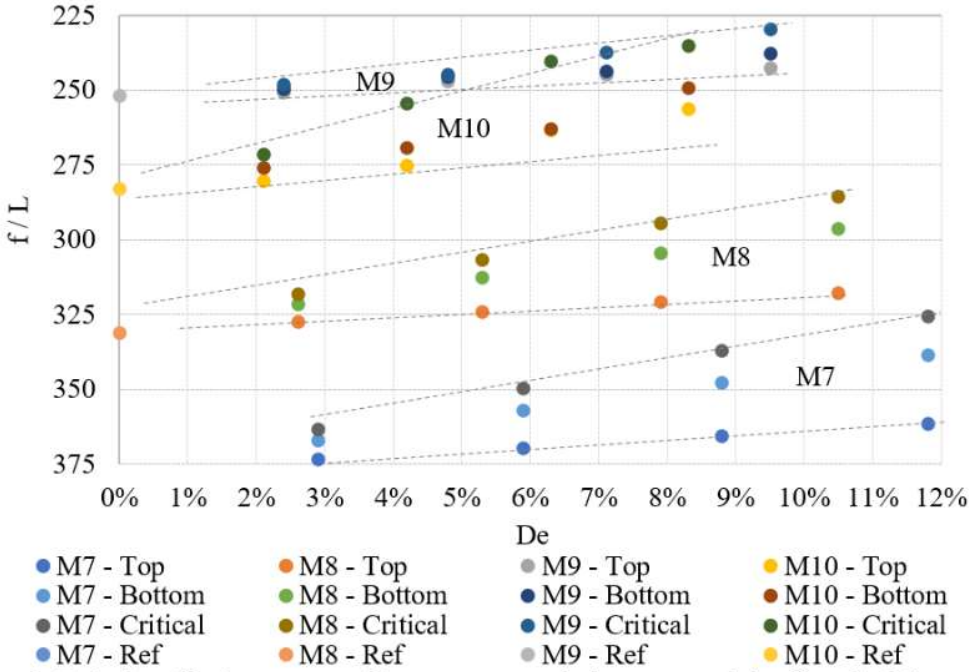

Figure 8. Relative displacement with respect to relative eccentricity for all slab models.

For slab models M9 and M10, the "Top", "Bottom" or "Critical" eccentricity positions had less of an effect than for models M7 and M8. The amplitude of variation of the center displacement increased as relative eccentricity increased. In the "Critical" case of model M9, the increase in relative eccentricity from 2.4% to 9.5% resulted in an increase in relative displacement from L/248 to L/230. For comparison, in the "Critical" case of model M7, the increase in relative eccentricity from 2.9% to 11.8% resulted in an increase in relative displacement from L/363 to L/325.

3.4 Load Balancing

Load balancing values increased when strands were inserted in order to attain the normal tensile stress limits at the top and bottom faces of the slab and in pre-compression. Table 8 shows a summary of load balancing values for all models. Only model M7 reached the recommended value between 60% and 80% of Loureiro (2006) and Aalami (2014). In the other models, load balance varied between 59% and 95% of permanent loads.

Revista ALCONPAT, 12 (2), 2022: 210 – 226

Table 8. Load balancing on all slab models (%).

Model		M7											
Case		Reference	Top				Bottom				Critical			
Hypothesis			0.5	1.0	1.5	2.0	0.5	1.0	1.5	2.0	0.5	1.0	1.5	2.0
Span	First	73	73	72	72	71	73	72	72	71	72	71	70	69
	Central	74	72	71	69	68	72	71	69	68	71	68	64	61
	Final	80	79	79	78	77	79	78	77	75	78	76	74	72
Model		M8											
Case		Reference	Top				Bottom				Critical			
Hypothesis			0.5	1.0	1.5	2.0	0.5	1.0	1.5	2.0	0.5	1.0	1.5	2.0
Span	First	82	81	80	79	78	81	80	78	77	80	78	75	73
	Central	92	89	87	84	82	89	87	84	82	87	82	77	72
	Final	87	87	86	85	84	86	84	83	81	85	82	80	78
Model		M9											
Case		Reference	Top				Bottom				Critical			
Hypothesis			0.5	1.0	1.5	2.0	0.5	1.0	1.5	2.0	0.5	1.0	1.5	2.0
Span	First	88	87	86	85	83	60	59	57	56	60	57	54	52
	Central	94	92	90	88	85	61	60	58	57	60	56	53	50
	Final	87	86	85	84	83	59	58	57	56	58	56	54	52
Model		M10											
Case		Reference	Top				Bottom				Critical			
Hypothesis			0.5	1.0	1.5	2.0	0.5	1.0	1.5	2.0	0.5	1.0	1.5	2.0
Span	First	97	96	95	94	93	95	93	91	89	94	91	88	85
	Central	93	92	90	88	86	92	90	88	86	90	86	83	79
	Final	88	87	87	86	85	87	95	83	81	86	83	80	77

3.5 Passive Reiforcement

Table 9 shows bottom passive reinforcement results for the slab models.

Table 9. Bottom passive reinforcement results

Model	Hypothesiss and Cases					
	Reference		H5 - Top		H5 - Bottom	
	First and Final span	Central span	First and Final span	Central span	First and Final span	Central span
	Steel area (cm²/m)		Steel area (cm²/m)		Steel area (cm²/m)	
M7	2.54	2.11	2.54	2.11	2.64	2.22
M8	2.72	2.10	2.72	2.10		
M9	3.26	2.40	3.26	2.40		
M10	3.74	2.46	3.74	2.46		

In the case of hypothesis H5 and "Top" case, bottom passive reinforcements were unchanged with respect to Reference values. Changes in reinforcement were observed within a model but in different spans.

Table 10. Top passive reinforcement results

Model	Hypothesis and Cases		
	Reference	H5 - Top	H5 - Bottom
	Steel area (cm²/m)		
M7	7.4	7.4	7.7
M8	10.5	10.5	
M9	12.2	12.2	
M10	15.6	15.6	

Table 10 shows results for the top passive reinforcement for all slab models. Similar to Table 9, the passive reinforcement rate used to cancel negative flexing remained unchanged for all models under hypothesis H5 and "Top" case with respect to Reference values. This was a consequence of the 5 mm reduction in height of the spacers over the pillars not inducing sufficient loads to demand an increase in steel. On the other hand, the variation of eccentricity in the "Bottom" case for model M7 resulted in an increase in reinforcement rate over the pillars to provide additional effect against negative flexing when compared to the Reference model with the same span.

4. CONCLUSIONS

This study analyzed four models of post-tensioned flat slabs with variations in the span between pillars and in strand eccentricity. The variations in eccentricity simulated errors in assembly and positioning of vertical spacers. Pre-compression stresses, normal tensile stresses in the top and bottom faces, load balancing and vertical displacements were analyzed. Top and bottom passive reinforcements were also analyzed.

A decrease in eccentricity of the strands had a direct effect on the slab loads: its main effect was a decrease in the ratio of normal stresses supported by post-tensioning. The decrease in eccentricity of the "Bottom" case had a stronger negative impact than a variation of eccentricity of the "Top" case and affected normal stress control, load balancing criteria and displacements.

Only model M7 with variations in eccentricity from hypothesis H5 were within limits set by standard NBR 6118 (ABNT, 2014) for the "Top" and "Bottom" cases. On other hand, models M8, M9 and M10, with variations in eccentricity from hypothesis H5 for the "Top" case presented normal tensile stresses below the 3.38 MPa limit of standard NBR 6118 (ABNT, 2014).

Pre-compression stresses in the structural element were affected only by the number of tendons and the load applied to them. There were no effects of variations in vertical height of spacers.

Vertical displacements of the slabs were affected by variations in eccentricity. Models M7 and M8 remained below the L/250 limit of standard NBR 6118 (ABNT, 2014) for all hypothesis of variations of eccentricity tested.

Load balancing criteria remained within recommended limits only for Model M7. However, since these criteria were complementary and not standardized, the other models could be acceptable for use nonetheless.

Reinforcement rate for top and bottom reinforcements were unchanged between the Reference model and all models with variations in eccentricity from hypothesis H5 and "Top" case.

The maximum variation of relative eccentricity so that the parameters of this study remained with established limits was 2.1% for the "Top" case. This was obtained by comparing the variation in eccentricity with respect to slab thickness.

Overall, results showed that flat post-tensioned slabs with unbonded tendons of type CP 190 RB, diameter of 12.7 mm and span between pillars between 7.0 m to 10.0 m could have a maximum

tolerance of 5 mm in a decrease of vertical height of strands in the top face of the slab ("Top" case). This result was more restrictive than found in reference studies.

5. REFERENCES

Aalami, B. O. (1990), *Load Balancing: A Comprehensive Solution to Post - Tensioning.* ACI Structural Journal: 662-670.

Aalami, B. O. (2014), *"Post-Tensioned Manual"*. California: ADAPT, v.1, p. 500.

Aalami, B. O. (2000*), Structural Modeling of Post-Tensioned Members*. Journal of Structural Engineering. Vol. 126 Nº. 2: 157-162.

Aalami, B. O., Bommer, A. (1999), *"Design Fundamntals of Post-Tensioned Concrete Floors"*. Post-Tensioning Institute (PTI), Farmington Hills, USA.

Almeida, S. R. M. (2001), "*Contribuição ao projeto ótimo de cabos em vigas de concreto protendido*". Tese de Doutorado. Pontifícia Universidade Católica do Rio de Janeiro. https://doi.org/10.17771/PUCRio.acad.2058.

American Concrete Institute (2019). *ACI 318 - Building Code Requirements for Structural Concrete.* Farmington Hills, MI.

Associação Brasileira de Normas Técnicas. (2019). *NBR 6120: Ações para o cálculo de estruturas de edificações*. Rio de Janeiro.

Associação Brasileira de Normas Técnicas. (2014). *NBR 6118: Projeto de estruturas de concreto – Procedimento*. Rio de Janeiro.

Caro, L. A., Vargas J. R. M., Ros, P. S. (2013), *Prestress losses evaluation in prestressed concrete prismatic specimens.* Engineering Structures. Vol. 48, p. 704-715. https://doi.org/10.1016/j.engstruct.2012.11.038.

Carvalho, R. C. (2017), "*Estruturas em concreto protendido: cálculo e detalhamento*". Ed. Pini. São Paulo, Brasil, p. 448.

Cauduro, E. L. (2002), *"Manual para a boa execução de estruturas protendidas usando cordoalhas de aço engraxadas e plastificadas"*. São Paulo, Brasil.

Cavaco, E. S., Bastos, A., Santos, F. A. (2017), *"Effects of corrosion on the behaviour of precast concrete floor systems"*. Journal Construction and Building Materials. N. 145: 411-418. https://doi.org/10.1016/j.conbuildmat.2017.04.044.

Cholfe, L., Bonilha, L. (2018), *"Concreto protendido: teoria e prática"*. Oficina de Textos. São Paulo, Brasil, p. 360.

Hanai, J. B. (2005), *"Fundamentos do Concreto Protendido"*. E-book. São Carlos.

Kang, T., Bondy, K. B. (2008), *Recommendations for Design of Post-Tensioned Slab-Column Connections Subjected to Lateral Loading.* PTI Journal, Post Tensioning Institute. Vol. 6, nº 1.

Loureiro, G. J. (2006), *Projeto de Lajes Protendidas com Cordoalhas Engraxadas.* Revista Ibracon de Estruturas e Materiais, ed. 44.

Pfeil, W. (1984), *"Concreto Protendido – Introdução"*. LTC. Rio de Janeiro.

Romanichen, R. M., Souza, R. A. (2019), *Reinforced concrete corbels strengthened with external prestressing.* Revista Ibracon de Estruturas e Materiais. V. 12. N. 4, p. 812 – 831. https://doi.org/10.1590/S1983-41952019000400006.

Santos, J. S. D. (2017), *"Desconstruindo o Projeto Estrutural de Edifícios: Concreto Armado e Protendido"*. 1ª. ed. São Paulo: Oficina de Textos. p. 127.

Silva, G., Prata, B., Albuquerque, A. (2018), *Análise da eficiência dos sistemas estruturais para edifícios em concreto.* Ambiente Construído. Vol. 18, n. 1, p. 313-325. https://doi.org/10.1590/s1678-86212018000100223.

Silva, R.C. (2003), *"Vigas de concreto armado com telas soldadas: análise teórica e experimental da resistência à força cortante e do controle da fissuração"*. Tese de doutorado. Escola de

Engenharia de São Carlos, Universidade de São Paulo. p. 328.
Silveira, M. C. A. (2002). *"Práticas de Projeto e Execução de Edificações Protendidas com Cordoalhas Engraxadas e Plastificadas"*. Revista Ibracon de Estruturas e Materiais. 44º Congresso Brasileiro do Concreto. Belo Horizonte.
Souza, F. A. (2018), *"Radier simples, armado e protendido – Teoria e Prática"*. Editora Catarse. São Paulo, Brasil, p. 312.
Souza Junior, O. A., Oliveira, D. R. C. (2016), *"Influence of the tendon´s layout on the shearing resistance of prestressed concrete beams"*. Revista Ibracon de estruturas e materiais. Vol. 9, N. 5. p. 765 – 795. https://doi.org/10.1590/S1983-41952016000500008.
Vicente, C. M. D. S., Albino, J. P. D. C. (1994), *"Lajes em Concreto Armado e Protendido"*. Editora da Universidade Federal Fluminense. Rio de Janeiro, Brasil, p. 584.
Xin, F., Xianyan, Z. (2012). *"Experimental research on crack width of retard bonded partially prestressed concrete beams"*. International Conference on Advances in Civil Infrastructure Engineering. Hunan.